# Delft University of Technology

# Fouling of ultrafiltration membranes by organic matter generated by marine algal species

Dhakal, Nirajan; Salinas-Rodriguez, Sergio G.; Ouda, Alaa; Schippers, Jan C.; Kennedy, Maria D.

**Important note**
To cite this publication, please use the final published version (if applicable).
Please check the document version above.

# Fouling of ultrafiltration membranes by organic matter generated by marine algal species

Nirajan Dhakal[a,b,*], Sergio G. Salinas-Rodriguez[a], Alaa Ouda[a], Jan C. Schippers[a],
Maria D. Kennedy[a,c]

[a] *IHE-Delft Institute for Water Education, Environmental Engineering and Water Technology Department, Westvest 7, 2611 AX Delft, The Netherlands*
[b] *Wetsus, European Centre of Excellence for Sustainable Water Technology, Oostergoweg 9, 8911 MA Leeuwarden, The Netherlands*
[c] *Delft University of Technology, Faculty of Civil Engineering, Stevinweg 1, 2628 CN Delft, The Netherlands*

## ABSTRACT

Controlling fouling in seawater reverse osmosis and ultrafiltration systems is a major challenge during algal blooms. This study investigates UF fouling potential of four marine algae and their algal organic matter (AOM): *Chaetoceros affinis (Ch), Rhodomonas balthica (Rh), Tetraselmis suecica (Te),* and *Phaeocystis globulosa (Ph).* Batch culture monitoring of the four different marine algal species showed remarkable differences in their production of biopolymers, transparent exopolymer particles (TEP) and their membrane fouling potential (MFI-UF$_{10\,kDa}$). MFI-UF$_{10\,kDa}$ was linearly related to biopolymer concentration, and TEP during the growth and stationary/death phase of all four algal species. But the linear relation of MFI-UF$_{10\,kDa}$ with algal cell density and chlorophyll-a concentration did not continue during the stationary/death phase. In experiments with capillary UF membranes, non-backwashable fouling of UF membranes varied strongly for the four different AOM solutions tested, and was linked to the presence of polysaccharides (stretching-OH) and sugar ester (stretching S=O) groups in the AOM. The non-backwashable fouling coincided with MFI-UF$_{150\,kDa}$ and TEP concentration. Therefore, determination of these parameters (MFI and TEP) and correlating with MODIS satellite data may generate useful information about the fouling potential of seawater at different locations during an algal bloom.

## 1. Introduction

Ultrafiltration (UF) is widely applied as pre-treatment in seawater reverse osmosis (SWRO) desalination plants [1–3]. The rationale behind the rapid expansion of UF at the expense of conventional pre-treatment systems is that it is very effective in removing particulate and colloidal matter ensuring permanently low silt density index (SDI) values. Since 2008, the use of UF as pre-treatment for SWRO has increased significantly [4]. However, controlling fouling in UF is a major challenge, in particular during seawater algal blooms [2,5].

Despite numerous advantages, the development of non-backwashable fouling resistance during algal blooms is a major threat to the operation of UF membranes in particular when in-line coagulation is not applied prior to UF [6]. During an algal bloom, algal cell density

and algal organic matter (released by algae) are responsible for membrane fouling [5]. Elevated levels of algal organic matter (AOM) drive the need for frequent hydraulic backwashing and chemical enhanced backwashing (CEB). Fouling compounds that adsorb or are tightly bound to the UF membrane are referred to as 'hydraulically irreversible' membrane fouling, and such fouling increases the frequency of CEB. To overcome these problems, conventional technologies are used to pre-treatment seawater e.g., in-line coagulation or dissolved air flotation (DAF) up front of UF. In general, UF pre-treatment with in-line coagulation is expected to be able to control UF fouling during algal blooms. However, environmental and sustainability considerations urge for minimizing/avoiding the use of chemicals in SWRO. Consequently, this study focuses on investigating fouling (caused by algal growth/blooms), of UF membranes operating without pre-treatment involving

coagulant dosing.

It has been shown that accumulation of algal organic matter (AOM) during algal blooms is the leading cause of membrane fouling, rather than the algal cells themselves [2,7–10]. The AOM consists of polysaccharides, proteins, lipids, nucleic acids, and other dissolved organic substances [11,12]. A fraction of AOM are transparent exopolymer particles (TEP) [13] which are very sticky polysaccharides and glycoproteins [14]. The TEP-like matter is expected to cause severe fouling in UF and RO systems and may even initiate biological fouling in RO systems [15–18]. To further develop strategies, preferably environmentally friendly, to control membrane fouling, the characteristics of the foulants need to be identified and monitored. Water quality parameters which potentially can be used to monitor UF fouling are algal cell density, chlorophyll-a and (algal) biopolymer concentration, transparent exopolymeric particles ($TEP_{10\,kDa}$) and membrane fouling potential ($MFI\text{-}UF_{10\,kDa}$).

The aim of this work is to study the fouling of ultrafiltration membranes by organic matter generated by marine algal species. For this purpose, four marine algal species namely *Rhodomonas balthica (Rh Chaetoceros affinis (Ch), Phaeocystis globulosa (Ph)* and *Tetraselmis suecica (Te)* were selected and cultured in the laboratory. The specific objectives are:

i. To monitor parameters potentially related to UF membrane fouling of AOM generated by four algal species during their growth and stationery/death phases.
ii. To investigate the relationship between UF membrane fouling potential (MFI-UF) of AOM and water quality parameters such as biopolymer concentration, TEP concentration, algal cell density and chlorophyll-a concentration.
iii. To establish the relationship between water quality parameters and backwashable and non-backwashable UF fouling rates by performing multi filtration cycles using AOM.
iv. To elucidate the AOM fractions that cause non-backwashable fouling of ultrafiltration membranes using Fourier Transform InfraRed (FTIR) spectroscopy.
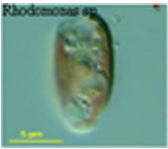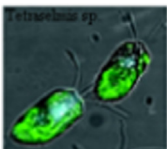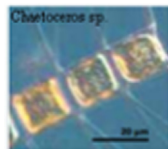
## 2. Material and methods

### 2.1. Characteristics of four algal species

The typical features of the four algal species are summarized in Table 1.

### 2.2. Algal cultures

Four strains of marine algal species were selected: Ch - diatom (CCAP 1010/27), Rh- cryptophyta (NIVA 5/91), Te-flagellates (CCAP 66/22),

and Ph-haptophytes (CCY 0801). These species were separately cultivated in 5 L glass bottles filled with natural North Sea water (TDS = 34 g/L, pH = 8 ± 0.3). Raw seawater was filtered through a 2 µm glass filter and autoclaved at 121 °C for 20 min and spiked with nutrients and trace elements based on the f/2 + Si and L1 Guillard's medium for Ch and Ph, respectively, while, Rh and Te were grown in f/2 Guillard's medium. The composition of the prepared media was described by Villacorte et al. [21]. Algal cultures, except Ph, were exposed to a continuous mercury fluorescent light at a controlled temperature of 20 ± 2 °C. However, algal culture Ph was exposed to 16 / 8 h light/dark regime, as this was expected to be optimal for its growth [22]. Aeration was provided to mix the solution and to have a continuous supply of oxygen. CO2 was added intermittently to adjust pH and for buffering [23]. The average algal cell and chlorophyll-a concentration in the batch cultures was monitored every 2 days (see Section 2.3). Additional samples were collected (also every 2 days) for LC-OCD (see Section 2.5.1), TEP (see Section 2.5.2) and modified fouling index (MFI-UF) measurements (see Section 2.5.5) until the stationary-death phase was reached.

### 2.3. Cell density and chlorophyll-a

The algal-cell density in batch cultures was monitored by sampling every two days and counting the cells using Haemacytometer (Burker-Turk counting chamber) slides and a light Nikon microscope (Olympus BX51). Flagellate-type of algal species were immobilized with Lugol's iodine solution before counting. Samples were also collected to measure chlorophyll-a according to the Dutch standard NEN 6520 protocol [24]. In short, the algal solution was filtered (GF 6 filter) and extracted with ethanol. The absorbance of the sample (before and after acidification with 0.4 M HCl) was measured at wavelengths of 665 and 750 nm using a spectrophotometer. The difference in absorbance of the solution is a measure of the chlorophyll-a concentration.

### 2.4. Extraction and characterization of algal organic matter (AOM)

Before using the water for further testing, samples were first allowed to settle for 24 h to remove the larger algal cells. Subsequently, the supernatant containing AOM was separated and filtered through a 5 µm polycarbonate filter (Nuclepore PC membranes, Whatman) with < 0.2 bars of vacuum. The filtered samples were analyzed using:

- Liquid chromatography - organic carbon detection (LC-OCD) (see Section 2.5.1)
- Transparent exopolymer particles ($TEP_{10\,kDa}$) (see Section 2.5.2).
- Fluorescence excitation-emission matrix (FEEM) spectroscopy (see Section 2.5.3)
- Fourier transform infrared (FTIR) spectroscopy (see Section 2.5.4)
- Modified fouling index ($MFI\text{-}UF_{10\,kDa}$) (see Section 2.5.5)

**Table 1**
Typical characteristics of the four algal species investigated this study.
Source [19,20]

| Characteristics | *Rh* | *Te* | *Ch* | *Ph* |
|---|---|---|---|---|
| |  |  |  |  |
| train | NIVA 5/91 | CCAP 66/22 | CCAP 1010/27 | CCY0801 |
| Type | Cryptophyta | Flagellates | Diatom | Haptophytes |
| Geometric shape | Cone + half sphere | Ovoid, slightly flattened | Oval cylinder | Spherical |
| Size | 8–12 µm | 9–11 µm | 8–10 µm | 3–8 µm |
| Colour | Reddish | Green | Golden brown | White |
| Strain origin | Baltic Sea | Pacific Ocean | Mediterranean Sea | North Sea |

The extracted AOM solution was used as a feed solution during UF experiments (see Section 2.7) and the backwashable and non-backwashable fouling rate development was calculated and compared.

## 2.5. Characterization techniques

### 2.5.1. Liquid chromatography - organic carbon detection (LC-OCD)

The biopolymer fraction of AOM extracted from the algal solutions was analyzed at Wetsus, Leeuwarden, the Netherlands using liquid chromatography organic carbon detection (LC-OCD). Before LC-OCD analyses, all samples were pre-filtered through 0.45 μm Millipore filters. Measurement and analysis of the samples was performed according to the protocol described by Huber et al. [25].

### 2.5.2. Transparent exopolymer particles (TEP_{10 kDa}) measurement

$TEP_{10 kDa}$ were measured according to the protocol described by Villacorte et al. [26]. In short, the water sample was filtered through a 10 kDa regenerated cellulose Millipore membrane filter, and the filtered volume ($V_f$) was measured. The retained TEP concentration on the filter paper was re-suspended in MilliQ water ($V_r$ = 10 mL) and stained with alcian blue (AB) that was pre-filtered through 0.05 μm polycarbonate filter. The TEP - AB solution (4 mL) was again filtered through a 0.1 μm polycarbonate filter at < 0.2 bar vacuum pressure. The absorbance ($A_e$) of the filtered sample and blank ($A_b$) were measured using a spectrophotometer at a wavelength of 610 nm. The $TEP_{10 kDa}$ concentration in mg Xanthan equivalent per liter was calculated using Eqs. (1) and (2).

$$TEP_{10 \ kDa} = f_{610nm} \frac{V_r}{V_f} (A_e - A_b) \tag{1}$$

$$f_{610nm} = \frac{1}{m_{610nm}} \tag{2}$$

where:

$f_{610 \ nm}$     Calibration factor [(mg-$X_{eq}$/L)/ (abs/cm)];
$m_{610 \ nm}$    Slope of the calibration line [(abs/cm)/ (mg-$X_{eq}$/L)]

### 2.5.3. Fluorescence excitation-emission matrix (FEEM) spectroscopy

The fluorescence emitting organic substances in AOM samples were measured using a FluoroMax-3 spectrophotometer (Horiba Jobin Yvon, Inc., USA) with a 150 W ozone-free xenon arc lamp to enable excitation. The AOM solutions were scanned over the excitation wavelength range from 240 to 450 nm, and an emission wavelength range of 290–500 nm to produce a three-dimensional matrix. Before FEEM analysis, the dissolved organic carbon (DOC) of AOM samples was measured using Shimadzu TOC, and diluted if necessary with MilliQ water to have a DOC concentration of approximately 1 mg/L. Excitation and emission matrices were analyzed using MatLab R 2011a, and the results were interpreted as described by Leenheer et al. [27].

### 2.5.4. Fourier transform infrared (FTIR) spectroscopy

FTIR spectroscopy was used to identify the functional groups present on the AOM fouled UF membranes before and after sonication (physical cleaning of the membrane). The AOM samples were first filtered using a flat sheet Millipore UF membrane (molecular weight cutoff, 10 kDa) at a constant flux of 60 L/m$^2$/h. The AOM-fouled membranes were analyzed using a PerkinElmer ATR – FTIR Spectrum-100 instrument at the Aerospace Engineering Laboratory of the Delft University of Technology. The AOM-fouled UF membrane was placed directly on the ATR crystal and held in place with a loading screw. An average of 16 scans between 4000 and 400 cm$^{-1}$ wavenumbers was recorded. The peak-picking feature of the spectrum analysis software was used to identify major peaks of interest.

The AOM-fouled UF membrane (after FTIR test) was placed in a clean disposable plastic container (40 mL) containing 10 mL of synthetic seawater. The samples were tightly covered and vortexed (Heidolph REAX 2000) for 10 s and sonicated (Branson 2510E-MT) for 90 min at 42 kHz to remove loosely bound AOM. The FTIR of the AOM-fouled UF membrane after sonication was compared with the FTIR results before sonication.

### 2.5.5. Modified fouling index (MFI - UF)

The modified fouling index (MFI - UF_{10 kDa}) was measured at constant flux through a membrane having pores of 10 kDa according to the protocol developed by Boerlage et al. [28] and modified by Salinas et al. [29]. Membranes having pores of 10 kDa were used because it is indicated/suggested that particles down to 10 kDa are likely responsible for particulate fouling of RO membranes. The water sample was filtered at a constant flux of 60 L/m$^2$/h using syringe pumps, and filter holder (Schleicher & Schuell). The pressure development over time was recorded using a pressure sensor. The data obtained for pressure versus time were plotted, and the minimum slope was calculated to determine the fouling index (I). MFI-UF was then calculated by normalizing the fouling index with standard reference values as proposed by Schippers and Verdouw [30] as Eq. (3).

$$MFI - UF = \frac{\eta_{20^oC} I}{2 \Delta P_o A_o^2} \tag{3}$$

where

$\eta_{20^oC}$    Water viscosity at 20 °C
$\Delta P$       Standard reference feed pressure (2 bars)
$A_o$       Standard reference membrane area of 13.8 × 10$^{-4}$ m$^2$.

### 2.5.6. Silt density index (SDI)

Silt density index is determined by measuring the rate of plugging of a 0.45 μm membrane filter at 2 bars according to the standard ASTM protocol [31]. The measurement is done as follows.

- time $t_1$ required to filter the first 500 mL is determined
- 15 min ($t_f$) after the start of this measurement, time $t_2$ needed to filter another 500 mL is determined
- SDI is calculated using the Eq. (4)

$$SDI = \frac{100 \quad \%}{t_f} \left(1 - \frac{t_1}{t_2}\right) = \frac{\% \quad P}{t_f} \tag{4}$$

The shorter time ($t_f$) has to be considered such as 10, 5, or 3 min if the plugging ratio (% P) exceeds 75%. The volume of filtered water sample is proportional to the diameter of the filter used.

### 2.5.7. MFI_{0.45}

The Modified fouling index (MFI _{0.45}) was developed by Schippers and Verdouw [30] and is based on the cake filtration model. For determination of MFI _{0.45}, the flow through the membrane filter is measured as a function of time.

$$\frac{t}{V} = \frac{\mu. R_M}{dP. A} + \frac{\mu. I}{2. \Delta P. A_M^2} V \tag{5}$$

where

$V$      filtrate volume (L or m$^3$)
$T$      time (s)
$A_M$    membrane area (m$^2$)
$dP$     applied pressure (Pa)
$\mu$      water viscosity (Pa s)
$R_M$    clean membrane resistance (m$^{-1}$)
$I$       fouling potential (m$^{-2}$)

The MFI _{0.45} is calculated from the slope of t/V versus V graph and is corrected for pressure and temperature.
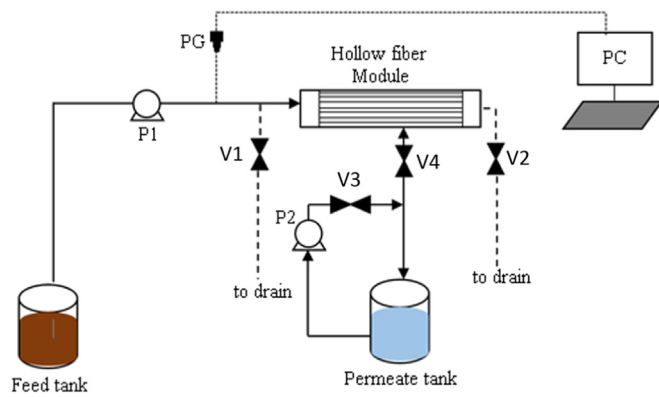
**Fig. 1.** Bench-scale filtration setup.

### 2.6. Preparation of ultrafiltration modules

Hollow-fiber polyethersulphone (PES) membranes (molecular weight cut-off, 150 kDa) obtained from Pentair X-Flow were used. The preparation of UF (pen) modules was according to the protocol of Tabatabai et al. [32]. In short, membrane pen modules were fabricated by potting four hollow fiber membranes with an internal diameter of 0.8 mm in a 30 cm transparent 8 mm outer diameter polyethylene tubing (Festo, Germany). Membrane modules were potted using polyurethane glue (Bison, the Netherlands). The effective surface area of the membrane was 30 cm² ± 2%. A new membrane pen module was used for each filtration experiment, and the prepared modules were soaked in 40 °C water for 24 h. All entrapped air, inside and outside the fibers, was removed before filtration experiments, and the modules were flushed with MilliQ water for 40 min prior to all experiments.

### 2.7. UF filtration experiments

Filtration experiments were performed using a bench-scale UF filtration unit in inside to outside mode at a flux of 80 L/m²/h (Fig. 1). A 20 min filtration cycle, followed by 45 s of backwashing with UF permeate at a flux of 200 L/m²/h was employed in the tests. During the filtration cycle, the valves V1 and V2 (Fig. 1) were closed while permeate valve V4 was open. During backwashing, all valves (V1, V2, V3 and V4) were open. The transmembrane pressure (TMP) development in each filtration cycle was recorded using a pressure sensor (Cerabar PMC 55, Endress and Hauser, Switzerland). The operational pressure range of Cerabar PMC 55 was 0–4 bars with a maximum deviation of 0.04%. The modem, FAX 195 Hart (Endress and Hauser, Switzerland) was connected to logged data on a computer.

Four different AOM solutions, originating from the four algal species, were used as feed solutions to the UF. The harvested AOM solutions were filtered through a 5 µm filter and diluted with North Seawater (which was filtered through a 2 µm filter and autoclaved at 121 °C for 20 min) to have a final biopolymer concentration of 0.5 ± 0.15 mg-C/L as a feed solution. Multi UF filtration cycles were performed for each AOM solution and development of transmembrane pressure over time was recorded. Assuming that cake/gel filtration is dominant in constant flux filtration, pressure development in UF membranes is given by Eq. (6).

$$\Delta P = \eta R_m J + \eta. \, I.J^2. \, t \tag{6}$$

where,

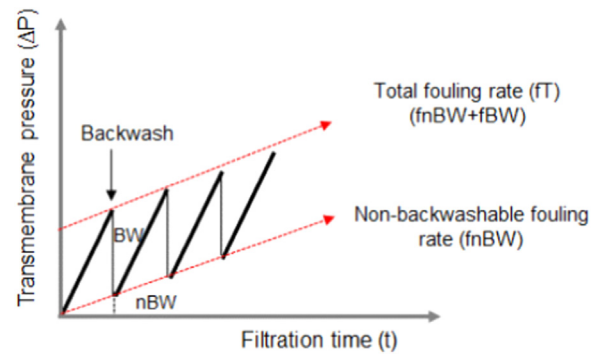| | |
|---|---|
| $\Delta P$ | is the applied pressure (bar) |
| $\eta$ | is viscosity (Pa s) |
| $R_m$ | is clean membrane resistance (m$^{-1}$) |
| $J$ | is filtration flux (L/m² h) |
| $I$ | is the fouling index (m$^{-2}$) |
| $t$ | is the filtration time (h) |



**Fig. 2.** Fouling development in constant flux dead-end UF systems.

Pressure (resistance to filtration) increases with filtration time until the membrane are cleaned by hydraulic backwashing. In many cases, backwashing is not effective in restoring the permeability and thus the pressure (resistance) increases after each successive filtration cycle. Total resistance due to fouling $R_t$ (m$^{-1}$) is the sum of backwashable ($R_{BW}$) and non-backwashable fouling resistance ($R_{nBW}$) and is given by Eq. (7)

$$R_t = R_{BW} + R_{nBW} = \frac{\Delta P}{\eta. \, J} \tag{7}$$

#### 2.7.1. Total, backwashable and non-backwashable fouling rate

Total, backwashable and non-backwashable fouling rates were calculated by plotting transmembrane pressure development as a function of (filtration) time (Fig. 2).

- **Non-backwashable fouling rate ($f_{nBW}$)** in bar/h is calculated using the slope of the TMP (the values of TMP directly after hydraulic backwashing were selected) versus filtration time.
- **Total fouling rate ($f_T$)** in bar/h is calculated using the slope of TMP (the values of TMP at the end of each filtration cycle/before hydraulic backwashing were selected) versus filtration time.
- **Backwashable fouling rate ($f_{BW}$)** in bar/h is calculated using Eq. (8).

$$\boldsymbol{f_{BW} = f_T - f_{nBW}} \tag{8}$$

where

| | |
|---|---|
| $f_T$ | total fouling rate (bar/h) |
| $f_{BW}$ | backwashable fouling rate (bar/h) |
| $f_{nBW}$ | non-backwashable fouling rate (bar/h) |

#### 2.7.2. Characterization of feed and permeate of UF membranes

LC-OCD analyses of all UF feed and permeate samples were performed. The rejection of biopolymers by UF membranes was determined and compared for all AOM solutions.

#### 2.7.3. Theoretical calculation of fouling potential of algal suspension

The fouling potential of algal suspension (without AOM) was calculated using the model Eq. (9) as described by [33].

$$\boldsymbol{MFI = \frac{15\pi d_P C_P}{\varphi^2} \frac{(1 - \epsilon)}{\in^3} \frac{\eta_{20^o C}}{\Delta P_o A_o^2}} \tag{9}$$

where:

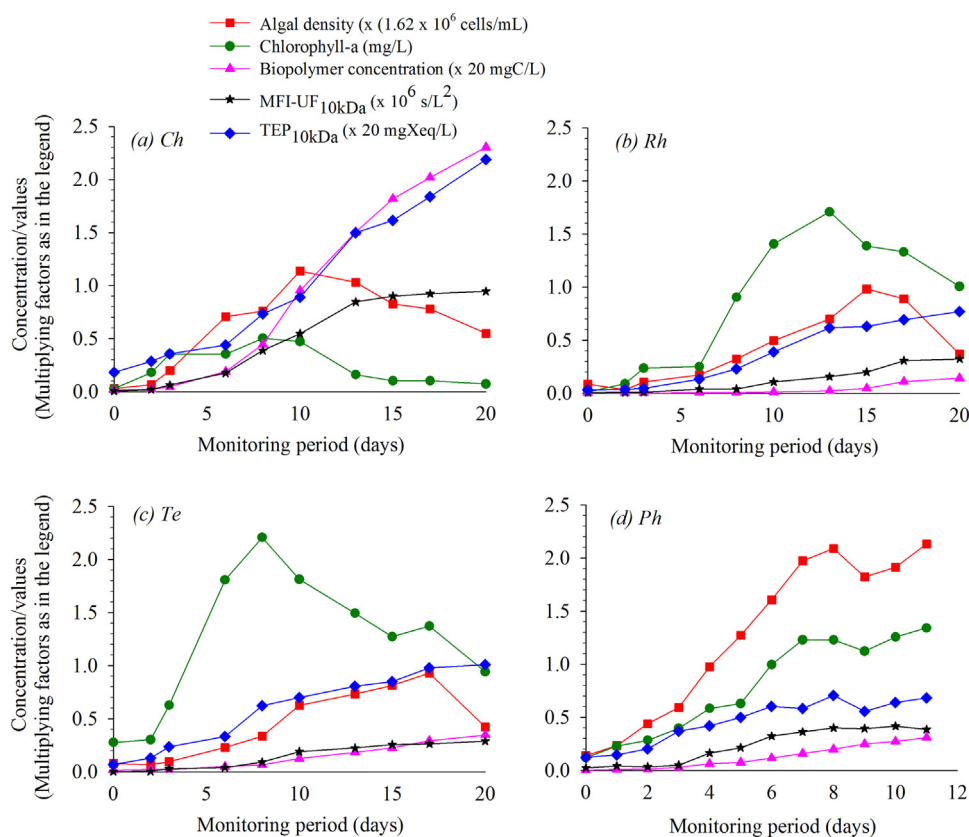| | |
|---|---|
| $\varepsilon$ | cake porosity |
| $\varphi$ | sphericity of the particles |
| $C_p$ | particle concentration (count/mL) |
| $d_p$ | diameter of particles in the cake |
| $\eta_{20\,°C}$ | water viscosity at 20 °C (0.001003 Pa s) |

**Fig. 3.** Development of algal cell density, MFI - UF, TEP, Chlorophyll a, Biopolymer concentration of batch cultures of (a) Ch, (b) Rh, (c) Te, and (d) Ph.

$\Delta P_0$    reference feed pressure (2 bar)
$A_0$      reference membrane area ($13.8 \times 10^{-4}$ m$^2$)

## 3. Results and discussion

### 3.1. Batch algal culture monitoring and fouling potential

Algal cell density, chlorophyll-a concentration, MFI-UF$_{10\,kDa}$, TEP$_{10\,kDa}$, and biopolymer concentration of four laboratory grown marine algal species were monitored (after inoculation) for a period of 21 (*Ch, Rh* and *Te*) and 11 days (*Ph*), respectively. The results are presented in Fig. 3 and each parameter monitored is discussed below.

### 3.1.1. Algal cell density and chlorophyll-a concentration

All four batch cultures varied in terms of their bloom duration, growth pattern and maximum concentration algal cell density and chlorophyll-a concentration. In addition, all algal species showed a lag phase of 1–2 days followed by an (exponential) growth phase, and a stationary/death phase. The *Ph* culture showed the maximum algal cell density ($3.4 \times 10^6$ cells/mL) on day 8 while *Ch, Rh* and *Te* recorded peak algal cell densities of $1.8 \times 10^6$ cells/mL (day 10), $1.8 \times 10^6$ cells/mL (day 15), and $1.8 \times 10^6$ cells/mL (day 17), respectively. The increase in algal cell density during the growth phase is attributed to the high level of nutrients in the solution. After the growth phase, a stationary/death phase was observed. In terms of chlorophyll-a, the highest concentration was recorded for *Te* (2200 µg/L) and the lowest for *Ch (500 µg/L)*.

The algal cell density and chlorophyll-a concentration reached were much higher than the levels which are indicative of an algal bloom in literature i.e. algal blooms are considered to occur when algal cell density exceeds 1000 cells/mL [34] and when chlorophyll-a concentration exceeds 10 µg/L [35]. Consequently, the solutions had to be diluted to a level, which is more likely to occur in practice. In this study,

a concentration of 0.5 mg-biopolymer-C/L was used as this concentration was measured in the North Sea during an algal bloom [33].

### 3.1.2. TEP$_{10\,kDa}$ and biopolymer concentration

Remarkable differences were observed in the concentration of TEP$_{10\,kDa}$ produced by the four algal species. In all cases, a very low concentration of TEP was measured in the lag phase (2–3 days) followed by a rapid increase during the growth and stationary/death phase. According to the results, the *Ch* culture produced the highest concentration of TEP$_{10\,kDa}$ (44 mg-Xeq/L), which was about 2–3 times higher than the *Rh, Te,* and *Ph* culture. The TEP concentration is higher than 1 mg-Xeq/L, which was observed by Villacorte in the North Sea [36]. In three cases, namely *Ch, Rh and Te* the biopolymer and TEP concentration and MFI-UF$_{10\,kDa}$ continued to increase even after at the stationary phase. This observation is attributed to the release of TEP from dead algal cells.

Likewise, remarkable differences were also observed among the four algal species regarding biopolymer concentration. The *Ch* culture produced the highest biopolymer concentration (46 mg/L), which was approximately 6, 8, and 15 times higher than cultures of *Te, Ph,* and *Rh*, respectively. The biopolymer concentration increased during the stationary/death phase, which could be due to cell lysis and release of intracellular organic matter in the solution [1,23]. Villacorte et al. [21] and Henderson et al. [37] also described a similar phenomenon for fresh and marine algal species.

### 3.1.3. Modified fouling index (MFI-UF$_{10\,kDa}$)

Among the four algal species, the culture of *Ch* showed the highest MFI-UF value (946,000 s/L$^2$), which was approximately 2–3 times higher than the cultures of *Rh, Te,* and *Ph*.

The maximum values of the measured parameters for the four algal species are presented in Table 2.

The specific MFI-UF$_{10\,kDa}$ is given in Table 3. These values show

**Table 2**

Maximum value of algal cell counts, chlorophyll-a, biopolymer, TEP concentration and MFI-UF of four marine algal species.

| Water quality parameters | Ch | Rh | Te | Ph |
|---|---|---|---|---|
| Algal cell ($\times 10^6$ cells/mL) | 1.8 | 1.6 | 1.5 | 3.4 |
| Chlorophyll-a (µg/L) | 503 | 1700 | 2200 | 1300 |
| Biopolymers (mg-C/L) | 46 | 3 | 7 | 6 |
| $TEP_{10\,kDa}$ (mg-Xeq/L) | 44 | 15 | 20 | 14 |
| MFI-UF$_{10\,kDa}$ ($\times$ 1000) s/L$^2$ | 946 | 324 | 290 | 417 |

**Table 3**

Specific MFI-UF$_{10\,kDa}$.

| MFI-UF$_{10\,kDa}$ ($\times 1000\ s/L^2$) | Ch | Rh | Te | Ph |
|---|---|---|---|---|
| Per $10^6$ algal cells | 526 | 203 | 193 | 123 |
| Per µg/L chlorophyll-a | 1,89 | 0,19 | 0,13 | 0,32 |
| Per mg-biopolymer-C/L | 21 | 108 | 41 | 70 |
| Per mg-Xeq/L $TEP_{10\,kDa}$ | 21 | 22 | 15 | 30 |

remarkable variations in chlorophyll-a and biopolymer concentration.

As illustrated in Fig. 4, the regression analysis performed showed that the biopolymer (polysaccharides and proteins) and TEP concentration were found to correlate with the MFI-UF$_{10\,kDa}$ during the growth phase and the stationary/death phase. This observation is attributed to the fact that biopolymer concentration, TEP, and MFI-UF continued to increase during the stationary/death phase of the algae as shown in Fig. 3. However, the relationship of MFI-UF$_{10\,kDa}$ with algal cell density and chlorophyll-a concentration was found poor during the stationary/death phase (see Supplementary Fig. 1) compared to the growth phase. This indicate that these parameters are not fully adequate to predict/quantify the fouling potential of RO (and UF) feed water during an algal bloom [2]. Consequently, continuous monitoring of algal cell densities and chlorophyll-a concentration, e.g., with MODIS satellite need to be complemented by recently developed parameters such as TEP, MFI-UF, and biopolymer concentration to get an adequate indication of the fouling properties of seawater during algal growth and

algal blooms.

Furthermore, to understand the role of algal cells, the fouling potential of algal suspensions without AOM was calculated using Eq. (9) based on assumptions for cake porosity ($\varepsilon$ = 0.4), sphericity of the particles ($\varphi$ = 1), and the average size of algal cells (3–12 µm) from Table 1. Other parameters such as algal cell density (Cp) were measured (Table 2). This theoretical calculation is just an indication of the MFI as it is very difficult to define the assumed parameters with algal suspensions due to their complexity, and it also very difficult to define the cake structure on a membrane. The consequence of these assumptions is that the MFI may be significantly underestimated.

The result illustrated in Table 4 shows that the MFI-UF values from experiments (algae and AOM) were much higher than theoretical calculation (with algae only). This indicates that the contribution of algal cells without AOM to the fouling potential is very low. However, it cannot be excluded that AOM, in particular, TEP, attached to algal cells, substantially increases the specific resistance of deposited algal cells and consequently contribute to the MFI-UF$_{10\,kDa}$.

### 3.2. Comparison of fouling potential of AOM and AOM plus algal cells

The fouling potential of AOM with and without algal cells was measured using parameters such as biopolymers, $TEP_{10\,kDa}$, MFI-UF$_{10\,kDa}$, MFI, and SDI (see Table 5). The AOM was separated from algal cells by pre-filtration of the sample through a 5 µm filter. The measured values of AOM without algal cells were significantly lower for all parameters when compared to AOM with algal cells. However, MFI 0.45 and SDI 3 of AOM + algal cells were not measured as the values exceeded the maximum theoretical value (for SDI 3 = 25) based on 75% plugging ratio. Consequently, the sample was diluted 50 times with synthetic seawater and re-measured, but this was only performed for the AOM solutions.

The lower fouling potential measured for AOM without algal cells suggested that a part of the AOM is attached to algal cells. Moreover, in practice, conventional full-scale pre-treatment such as micro straining followed by coagulation/flocculation and sedimentation or dissolved air flotation or micro straining followed by inline coagulation is
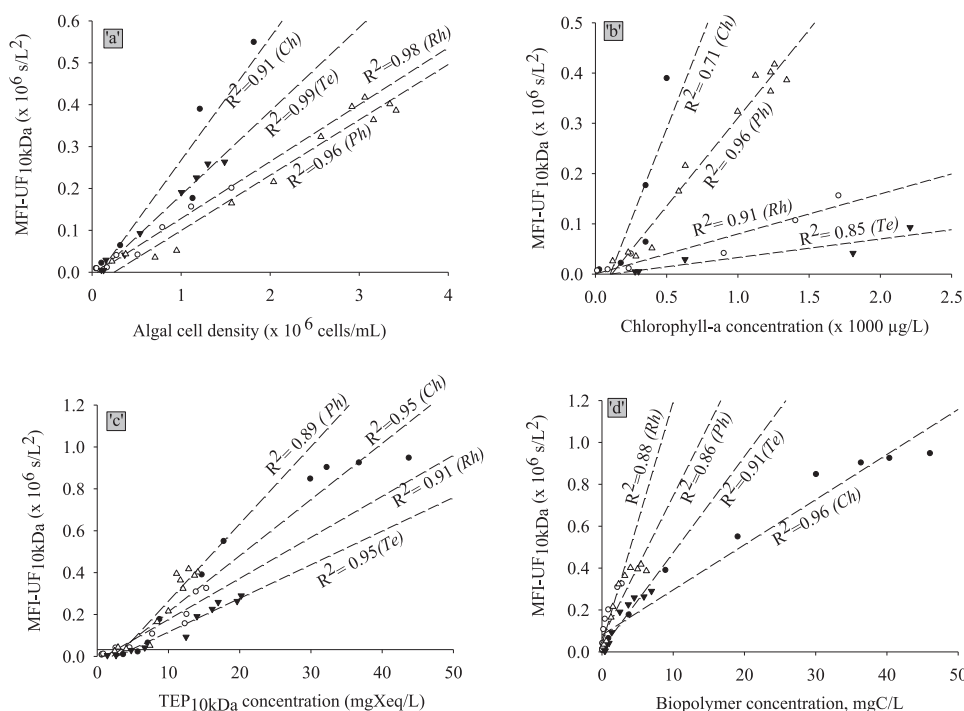


**Fig. 4.** Correlation between membrane fouling potential and algal cell density, chlorophyll-a concentration, TEP concentration, and biopolymer concentration during the growth phase of four algal species Ch, Rh, Te, &Ph.

**Table 4**
Measured and calculated MFI-UF.

| Algal species | Shape | Average size, μm | Algal cells density (cells/mL) | Measured[a](MFI-UF s/L$^2$) Algae + AOM | Calculated[b](MFI-UF s/L$^2$) Algae |
|---|---|---|---|---|---|
| *Ch* | Oval cylinder | 9 | 1800,000 | 946,000 | 19 |
| *Rh* | Cone | 10 | 1600,000 | 324,000 | 22 |
| *Te* | Ovoid | 10 | 1500,000 | 290,000 | 17 |
| *Ph* | Spherical | 6 | 3400,000 | 417,000 | 24 |

[a] Calculated from experimental data (batch cultures).
[b] Calculated from theoretical data: ε = 0.4, φ = 1, dp = average size of algal species, Cp = algal cell density, cells/mL.

expected to remove large particles such as algal cells prior to UF. Thus, studying the fouling potential of AOM (without algal cells) may provide a more realistic picture of the fouling potential in a full scale UF-SWRO plant. Therefore, in this study, AOM after filtration through a 5 μm filter was used a feed solution during UF experiments.

### 3.3. Characterization of algal organic matter (AOM)

#### 3.3.1. Liquid chromatography – organic carbon detection (LC-OCD)

The organic carbon detector (OCD) chromatograms of four AOM samples obtained from LC-OCD analysis are presented in Fig. 5a. Two distinct peaks were observed in the chromatogram. The peak that eluted approximately at 32–35 min after the sample injection into the system was assigned to the biopolymer fraction of organic carbon (high molecular weight > 20 kDa) which comprises proteins and polysaccharides. A remarkable difference was observed in the peaks of the biopolymer fraction of the four different cultured AOM solutions. In terms of absolute concentration, AOM of *Ch* has the highest biopolymer concentration (14.6 mg-C/L), which is approximately 4, 17 and 20 times higher than AOM of *Te*, *Rh*, and *Ph*, respectively (Fig. 5b).

The second peak that eluted between 45 and 55 min was assigned to building blocks and humic substances. These peaks might have originated entirely from the medium, i.e., EDTA added to the algal culture, which was used as a chelating agent to minimize the precipitation of metals in the medium. The LC-OCD analysis of EDTA showed a peak at a retention time (50–57 min) [21] similar to the elution time for building blocks and humic substances (result not shown here).

#### 3.3.2. Fluorescence excitation-emission matrix (FEEM)

The FEEM spectra were performed on the AOM solutions. As illustrated in Fig. 6, both protein-like and humic-like peaks were identified in the FEEM spectra of AOM of the four algal species. In all cases, the observed fluorescence intensity of the protein-like peak (i.e., mainly originating from tyrosine-like proteins - P1) was higher than the humic-like peaks (H1 and H2).

### 3.4. Fouling behavior of AOM generated by the four algal species in UF

Fig. 7 shows the development of transmembrane pressure (TMP) versus time during UF filtration cycles at a flux of 80 L/m$^2$ h and a feed solution containing a biopolymer concentration of 0.5 mg-C/L. As illustrated in Fig. 7, the AOM of *Rh* and *Ch* showed a very fast increase in total fouling as well as non-backwashable fouling resistance during consecutive filtration cycles in comparison to the AOM of *Te* and *Ph*. From these curves, the total and non-backwashable fouling rate was calculated (Table 6). The non-backwashable fouling resistance calculated based on initial transmembrane pressure (TMP) values after backwashing of each filtration cycle are presented in Fig. 8.

From Fig. 8, the percentage increase in non-backwashable fouling resistance ($R_{nBW}$) after 120 min of filtration was calculated and compared for all four AOM solutions. Accordingly, the percentage increase in $R_{nBW}$ was 254%, 208%, 83%, and 51%, respectively for *Rh, Ch, Te,* and *Ph*. This was also supported by the specific TEP concentration (mg-Xeq/L)/(mg-biopolymer- C/L) (calculated in Table 6), which reflects the concentration of TEP per mg biopolymer carbon concentration and was highest for *Rh* (4.6 mg-Xeq/L/mg-biopolymer- C/L) followed by *Ch* (2.2 mg-Xeq/L/mg-biopolymer- C/L), Te (1.9 mg-Xeq/L/mg-biopolymer- C/L) and Ph (1.0 mg-Xeq/L/mg-biopolymer- C/L). These result suggest that non - backwashable fouling in UF varied strongly with the type of algal species and AOM they produced. The non - backwashable fouling in UF also coincided with MFI-UF$_{150\,kDa}$ and specific TEP concentration (Table 6) and the higher these levels, the higher the non-backwashable fouling.

#### 3.4.1. Nature of AOM deposited on UF membranes

Fig. 9 shows FTIR spectra of a virgin and a fouled UF membrane before and after sonication. Table 7 presents the functional groups based on the IR spectra and the typical organic compounds associated with AOM [21,38].

All AOM fouled UF membranes show the broad and intense band of stretching (O - H group) at a wavelength of 3400–3200 cm$^{-1}$ (Peak A). This band could be due to the presence of carboxylic acids, alcoholic and phenolic compounds usually associated with polysaccharides [38]. The stretching refers to the change in inter-atomic distance along the bond axis and bending refers to the change in the angle between two bonds. Another peak (F) observed at a wavelength of 1280–1200 cm$^{-1}$ corresponds to C - O stretching, and OH deformation of -COOH is an indication of the presence of polysaccharides as well. Likewise, several other observed peaks (C, D, and E) in the wavelength range from 1650–1480 cm$^{-1}$ are mostly associated with the presence of proteins. Peak G indicates the presence of CH aromatic compounds possibly originating from humic-like substances. Peak H shows intense

**Table 5**
Measured MFI - UF, TEP, biopolymer concentration for AOM + algal solution, and AOM solutions.

| Algal species | Biopolymers (mg-C/L) | | TEP$_{10\,kDa}$ (mg-Xeq/L) | | MFI-UF$_{10\,kDa}$ (s/L$^2$ ×1000) | | MFI $_{.45}$ (s/L$^2$)[a] | | SDI3[a] | |
|---|---|---|---|---|---|---|---|---|---|---|
| | A | B | A | B | A | B | A | B | A | B |
| *Ch* | 46.0 | 14.6 | 43.8 | 19.8 | 946 | 369 | nm | 110 | > 25 | 24.6 |
| *Rh* | 2.8 | 0.9 | 15.4 | 8.9 | 324 | 177 | nm | 80 | > 25 | 22.6 |
| *Te* | 7.0 | 4.0 | 20 | 15.8 | 290 | 272 | nm | 60 | > 25 | 22.5 |
| *Ph* | 6.0 | 0.7 | 13.4 | 3.2 | 386 | 21 | nm | 50 | > 25 | 18.6 |

A = AOM with algal cells, B = AOM without algal cells, nm = not measured.
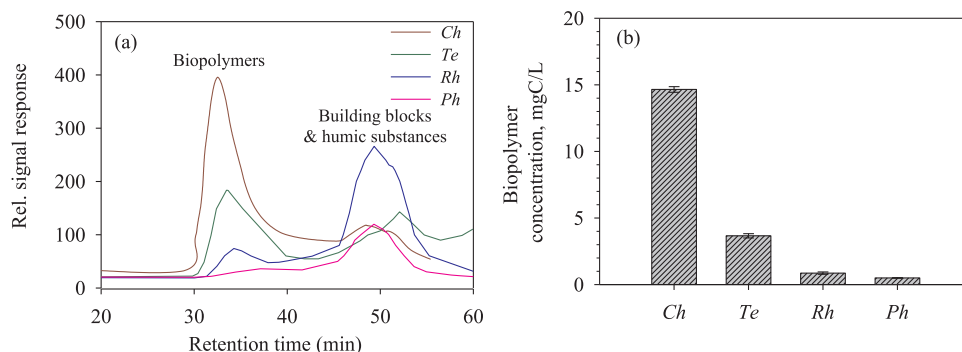[a] Samples were 50 times diluted with filtered seawater.

**Fig. 5.** a) LC - OCD chromatograms of AOM extracted during the stationary/decline phase of the four marine algal species. b) Concentration of biopolymer measured in four algal AOM.

absorption bands at $1050\,cm^{-1}$, which correspond to $-\,S = O$ stretching of sugar ester sulphate groups.

In general, the FTIR spectra findings were consistent with what was reported in marine mucilage aggregates by Mecozzi et al. [38] and for freshwater and seawater AOM by Villacorte et al. [21]. The spectra show the presence of polysaccharides, proteins, and humic substances which were also consistent with the findings of LC-OCD and F-EEM analyses.

After sonication, absorbance (peak height) was largely reduced for most peaks. Two broad and intense high peaks (A and H) linked to polysaccharides and sugar ester sulphates, respectively were partly re-duced even after extended sonication. The reduction in most peaks of fouled UF membranes after sonication (physical cleaning) was better in

the case of AOM of *Te* and *Ph* than in the case of AOM of *Rh* and *Ch*. This indicates that the adherence of AOM to the membrane surface was different for the different algal species. Consequently, non-back-washable of UF membranes during algal blooms will be governed by the characteristics of the AOM, which depend on the algal species present. Rehmana et al. [10] also highlighted that the production and compo-sition of dissolved AOM varied depending on algal species and their growth stage.

### 3.4.2. Passage of biopolymers through UF membranes

As illustrated in Fig. 10, the percentage passage of the biopolymer fraction of AOM through UF membranes ranged from 20% to 40%. This finding indicates that some biopolymers are smaller than the pores of
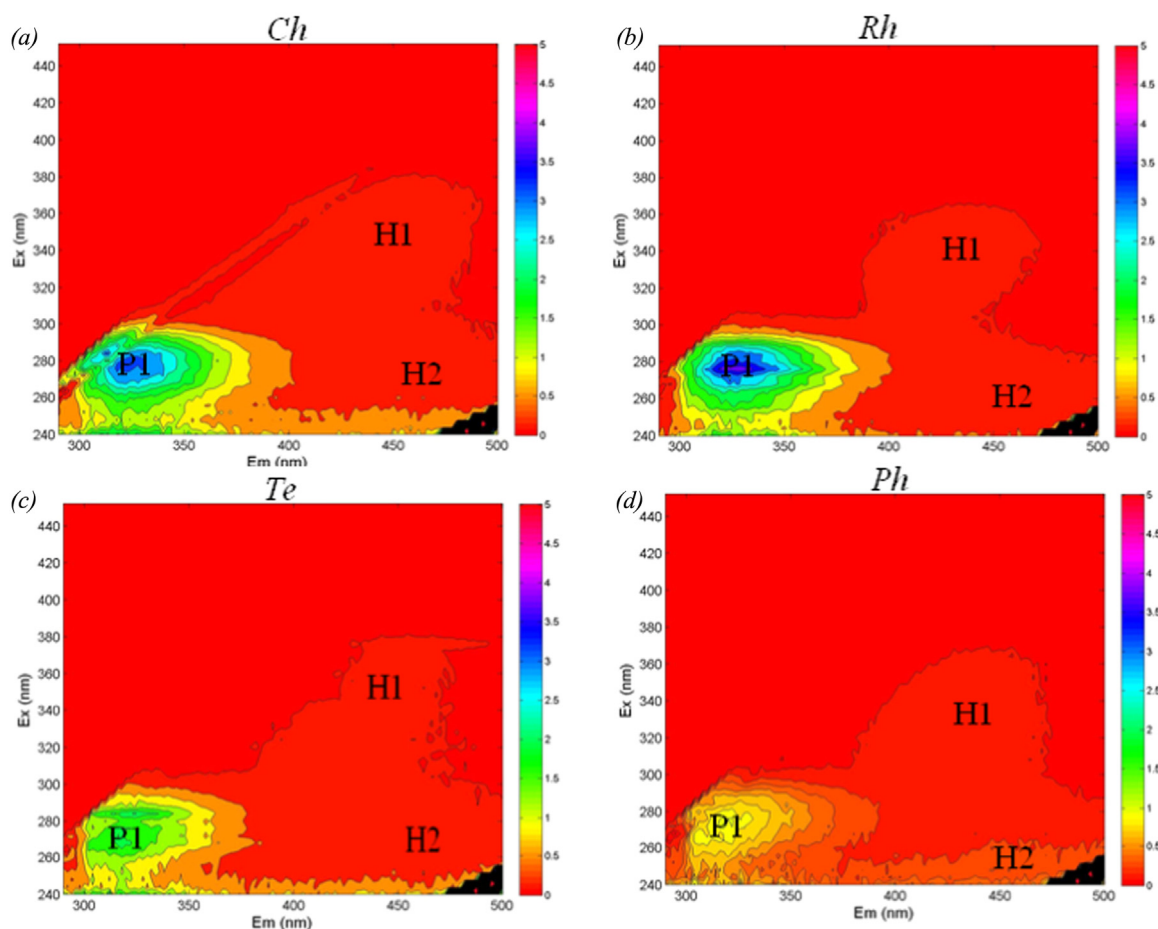


**Fig. 6.** Typical FEEM spectra prepared using Matlab for AOM samples of four algal species a) Ch. b) Rh. c) Te. and d) Ph. Legend: H1 = primary humic-like peak; H2 = secondary humic-like peak and P1 = tyrosine-like protein peak.
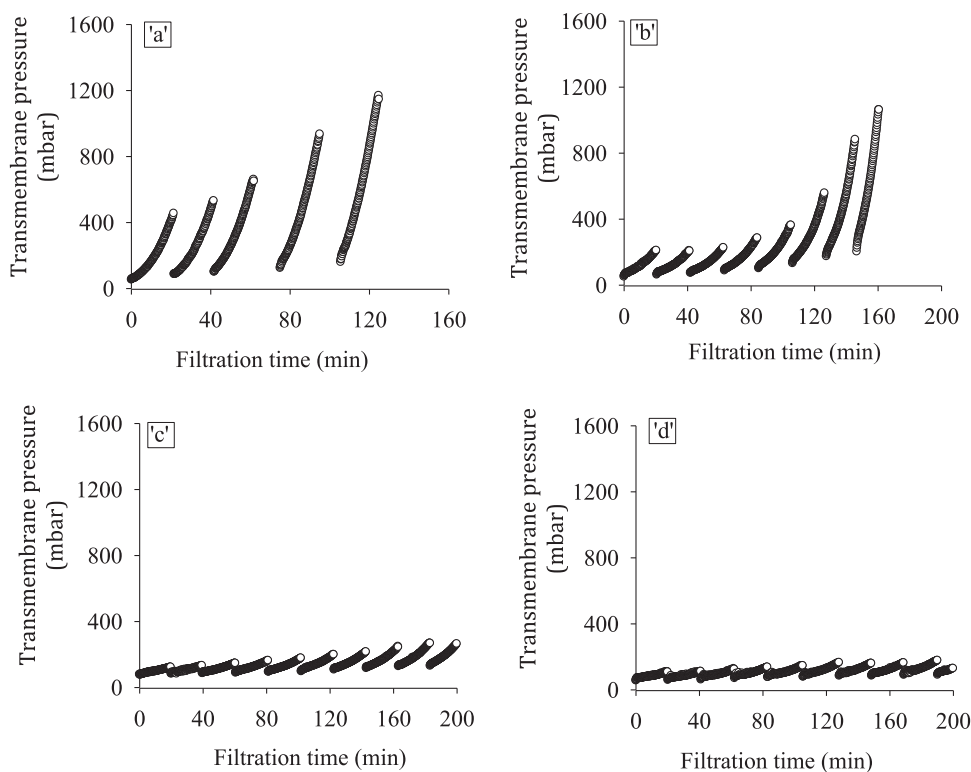
**Fig. 7.** TMP development during multiple UF cycles with AOM ($C_{feed}$ = 0.5 mg-biopolymer-C/L and flux = 80 L/m$^2$ h) from four different marine algal species (a) Ch, (b) Rh, (c)Te, and (d) Ph.

**Table 6**
Fouling parameters (MFI-UF), TEP, fouling rate development, and % increase in non-backwashbale resistance (Flux = 80 L/m$^2$ h, feed biopolymer concentration ~ 0.5 mg-C/L).

| Algal species | [a]MFI − UF$_{150 kDa}$ (s/L$^2$ × 1000) | Specific TEP(mg-Xeq/L /mg-biopolymer C/L) | Total fouling rate ($f_T$), (bar/h) | Δp (mbar) | | Non-backwashable resistance ($R_{nBW}$)(m$^{-1}$) | | | % increase in $R_{nBW}$ |
|---|---|---|---|---|---|---|---|---|---|
| | | | | at t = 0 | at t = 120 min (after BW) | at t = 0 (x10$^{11}$) | at t = 120 min (after BW) (x10$^{11}$) | dR$_{nBW}$ (x10$^{11}$) | |
| Rh | 46 | 4.6 | 0,37 | 48.6 | 172.3 | 2.4 | 8.0 | 5.7 | 254 |
| Ch | 26 | 2.2 | 0,53 | 51.5 | 158.7 | 2.2 | 7.4 | 5.0 | 208 |
| Te | 9 | 1.9 | 0,14 | 57.7 | 105.9 | 2.7 | 4.9 | 2.2 | 83 |
| Ph | 1 | 1.0 | 0,03 | 54.6 | 82.7 | 2.3 | 3.4 | 1.2 | 51 |

[a] Calculated based on the minimum slope of the first filtration cycle, BW = backwashing.



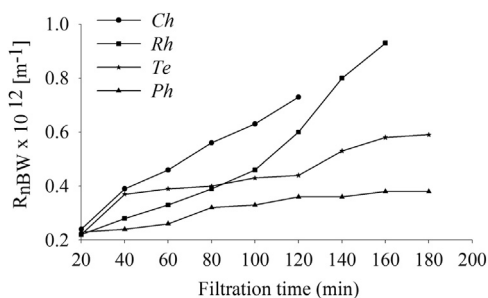**Fig. 8.** Non-backwashable fouling resistance development during multiple UF cycles with AOM ($C_{feed}$ = 0.5 mg-biopolymer-C/L and flux = 80 L/m$^2$ h) from four different marine algal species (a) Ch, (b) Rh, (c)Te, and (d) Ph.

UF membranes. Consequently, it cannot be excluded that a part of these compounds might contribute to pore fouling/blocking resulting in non-backwashable fouling of UF membranes.

## 4. Conclusions

- During the growth and stationary/death phase of four different marine algal species, MFI-UF$_{10 kDa}$ correlated linearly with biopolymer and TEP concentration. However, there was no correlation between MFI-UF$_{10 kDa}$ and algal cell density or chlorophyll-a concentration during the stationary/death phase.
- Substantial differences in the production of biopolymers and TEP were observed between the four algal species.
- The specific membrane fouling potential measured as MFI-UF$_{10 kDa}$ per mg biopolymer C/L for the different algal species varied by a factor 5.
- The measured MFI-UF$_{10 kDa}$ is attributed to the biopolymer/TEP concentration and not to the algal cell concentration. However, biopolymers/TEP attached to the algal cells may contribute (substantially) to the MFI-UF.
- Non - backwashable fouling varied strongly with the type of algal species and coincided with MFI-UF$_{150 kDa}$ and specific TEP concentration. The higher these levels, the higher the non-backwashable fouling. AOM from Rh and Ph showed the highest and the lowest non-backwashable fouling, respectively.
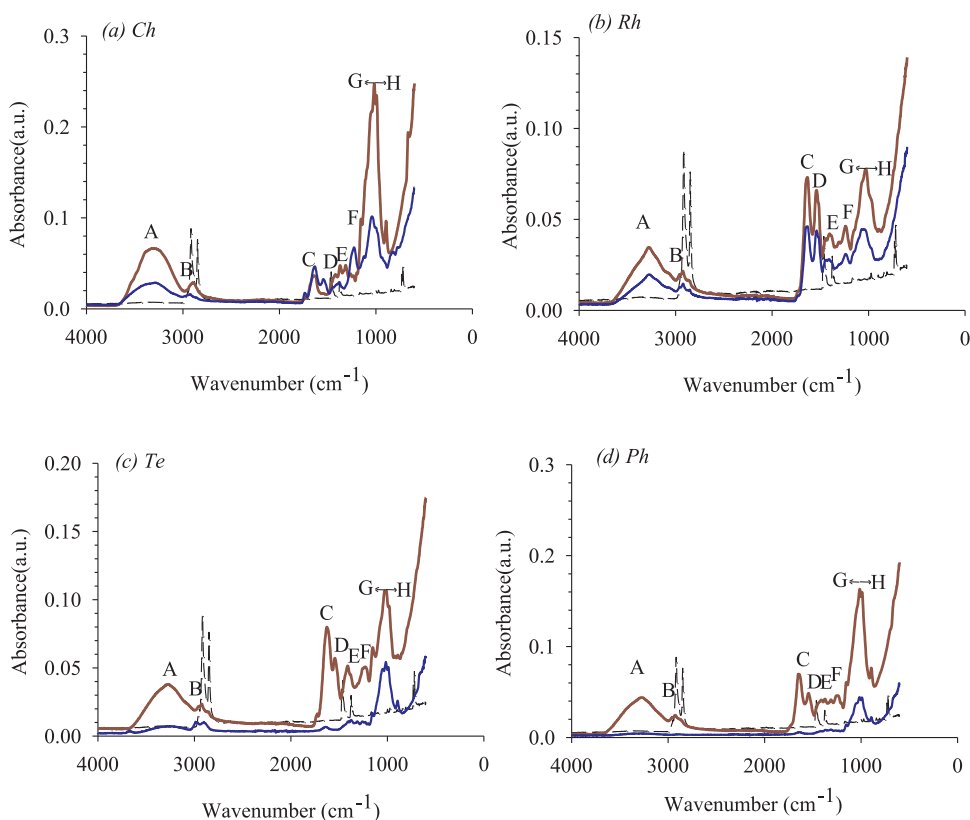
**Fig. 9.** FTIR spectra of AOM-fouled UF membrane samples for Ch, Rh, Te, and Ph. a) Solid line (red) represents the FTIR Spectra for AOM-fouled UF before sonication, b) Solid line (blue) represents the FTIR Spectra for AOM-fouled UF after 90 min of sonication at 42 kHz, and c) dotted line represents FTIR Spectra for virgin UF membrane.

**Table 7**

Absorption band, functional group and compound identified in FTIR test of AOM fouled UF.

| Peak | Wavelength (cm$^{-1}$) | Functional group | Compound |
|------|------------------------|------------------|----------|
| A | 3400–3200[a] | Stretching OH | Polysaccharides |
| B | 2950–2850[b] | Stretching CH$_2$ | Lipids |
| C | 1650–1640[a] | Stretching C = O and C - N (Amide I) | Proteins |
| D | 1545–1540[b] | Stretching C - N & bending NH (Amide II) | Proteins |
| E | 1500–1480[b] | C - N stretch and bend | Proteins |
| F | 1280–1200[b] | Stretching C - O & OH deformation of COOH | Polysaccharides |
| G | 1080–1070[a] | CH aromatic | Humic substances |
| H | 1050[a] | Stretching – S = O | Sugar ester sulphates |

Interpretation of IR spectra was based on Mecozzi et al. [38] and Villacorte et al. [21].

[a] Intense band.
[b] Weak band.

- Non-backwashability was attributed to - OH groups present in polysaccharides and – S = O sugar ester groups present in biopolymers.
- 60 – 80% of biopolymers were rejected by UF (150 kDa MWCO) depending on the algal species.

## 5. Recommendations

- Determining MFI-UF$_{10\,kDa}$, biopolymer, and TEP concentration, during algal blooms, and correlating with the MODIS satellite will generate useful information about the fouling potential of seawater at different locations.
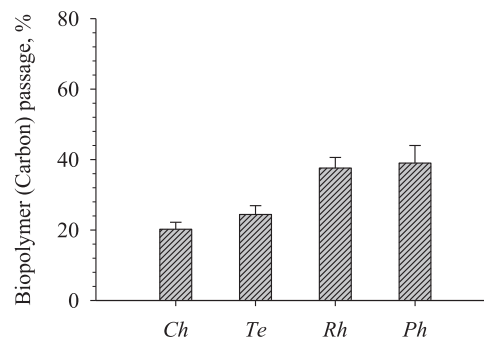


**Fig. 10.** Percentage of biopolymer passage through UF membranes (150 kDa) for AOM of four different algal species fed at a concentration of 0.5 mg-biopolymer-C/L and operated at a flux of 80 L/m$^2$ h.

## Appendix A. Supporting information

Supplementary data associated with this article can be found in the online version at http://dx.doi.org/10.1016/j.memsci.2018.03.057.

## References

[1] N. Voutchkov, Considerations for selection of seawater filtration pretreatment system, Desalination 261 (2010) 354–364.

[2] L.O. Villacorte, Y. Ekowati, H. Winters, G. Amy, J.C. Schippers, M.D. Kennedy, MF/UF rejection and fouling potential of algal organic matter from bloom-forming marine and freshwater algae, Desalination 367 (2015) 1–10.

[3] V. Bonnélye, L. Guey, J. Del Castillo, UF/MF as RO pre-treatment: the real benefit, Desalination 222 (2008) 59–65.

[4] J. Arevalo, M.D. Kennedy, S.G. Salinas-Rodriguez, R. Sandin, F. Rogalla, V.M. Monsalvo, Pretreatment systems in desalination plants to reduce extreme events impact in drinking water production., in: Proceedings of Pan-European Symposium Water and Sanitation Safety Planning and Extreme Weather Events, Bilthoven, Netherlands, 2017.

[5] D.A. Caron, M.-È. Garneau, E. Seubert, M.D.A. Howard, L. Darjany, A. Schnetzer, I. Cetinić, G. Filteau, P. Lauri, B. Jones, S. Trussell, Harmful algae and their potential impacts on desalination operations off southern California, Water Res. 44 (2010) 385–416.

[6] R. Schurer, A. Tabatabai, L. Villacorte, J.C. Schippers, M.D. Kennedy, Three years operational experience with ultrafiltration as SWRO pre-treatment during algal bloom, Desalin. Water Treat. 51 (2013) 1034–1042.

[7] D.A. Ladner, D.R. Vardon, M.M. Clark, Effects of shear on microfiltration and ultrafiltration fouling by marine bloom-forming algae, J. Membr. Sci. 356 (2010) 33–43.

[8] F. Qu, H. Liang, J. Tian, H. Yu, Z. Chen, G. Li, Ultrafiltration (UF) membrane fouling caused by cyanobacteria: fouling effects of cells and extracellular organics matter (EOM), Desalination 293 (2012) 30–37.

[9] R. Schurer, A. Janssen, L.O. Villacorte, M.D. Kennedy, Performance of ultrafiltration & coagulation in an UF-RO seawater desalination demonstration plant, Desalin. Water Treat. 42 (2012) 57–64.

[10] Z.U. Rehmana, S. Jeonga, T. S.A.A, A.H. Emwasb, T. Leiknesa, Advanced characterization of dissolved organic matter releasedby bloom-forming marine algae, Desalin. Water Treat. 69 (2017) 1–11.

[11] G. Fogg, The ecological significance of extracellular products of phytoplankton photosynthesis, Bot. Mar. 26 (1) (1983) 1–43.

[12] S.M. Myklestad, Release of extracellular products by phytoplankton with special emphasis on polysaccharides, Sci. Total Environ. 165 (1995) 155–164.

[13] L.O. Villacorte, Y. Ekowati, H. Winters, G. Amy, J.C. Schippers, M.D. Kennedy, Characterisation of transparent exopolymer particles (TEP) produced during algal bloom: a membrane treatment perspective, Desalin. Water Treat. 51 (2013) 1021–1033.

[14] U. Passow, A.L. Alldredge, A dye-binding assay for the spectrophotometric measurement of transparent exopolymer particles (TEP), Limnol. Oceanogr. 40 (1995) 1326–1335.

[15] T. Berman, M. Holenberg, Don't fall foul of biofilm through high TEP levels, Filtr. Sep. 42 (2005) 30–32.

[16] T. Berman, R. Mizrahi, C.G. Dosoretz, Transparent exopolymer particles (TEP): a critical factor in aquatic biofilm initiation and fouling on filtration membranes, Desalination 276 (2011) 184–190.

[17] M.D. Kennedy, F.P. Muñoz - Tobar, G.L. Amy, J.C. Schippers, Transparent exopolymer particles (TEP) fouling of ultrafiltration membrane systems, Desalin. Water Treat. 6 (1–3) (2009) 169–176.

[18] S. Li, H. Winters, L.O. Villacorte, Y. Ekowati, A.-.H.M. Emwas, M.D. Kennedy, G.L. Amy, Compositional Similarities and Differences between Transparent Exopolymer Particles (TEP) from two Marine Bacteria and two Marine Algae: Significance to Surface Biofouling, Marine Chemistry.

[19] 〈http://www.ccap.ac.uk/ccap-search.php〉, Culture collection of algae and protozoa, in.

[20] 〈http://nordicmicroalgae.org/taxon/Rhodomonas%20baltica〉, Nordic microalgae and aquatic protozoa, in.

[21] L.O. Villacorte, Y. Ekowati, T.R. Neu, J.M. Kleijn, H. Winters, G. Amy, J.C. Schippers, M.D. Kennedy, Characterisation of algal organic matter produced by bloom-forming marine and freshwater algae, Water Res. 73 (2015) 216–230.

[22] D. M, Personal. Commun. (2014), 〈http://www.zeeschelp.nl/〉.

[23] T. Merle, L. Dramas, L. Gutierrez, V. Garcia-Molina, J.-P. Croué, Investigation of severe UF membrane fouling induced by three marine algal species, Water Res. 93 (2016) 10–19.

[24] N.S.I, NEN, NEN 6520:2006- NL, Water – spectrophotometric determination of chlorophyll-a content, 2006.

[25] S.A. Huber, A. Balz, M. Abert, W. Pronk, Characterisation of aquatic humic and non-humic matter with size-exclusion chromatography – organic carbon detection – organic nitrogen detection (LC-OCD-OND), Water Res. 45 (2011) 879–885.

[26] L.O. Villacorte, Y. Ekowati, H.N. Calix-Ponce, J.C. Schippers, G.L. Amy, M.D. Kennedy, Improved method for measuring transparent exopolymer particles (TEP) and their precursors in fresh and saline water, Water Res. 70 (2015) 300–312.

[27] J.A. Leenheer, J.-P. Croué, Peer reviewed: characterizing aquatic dissolved organic matter, Environ. Sci. Technol. 37 (2003) 18A–26A.

[28] Ś.F.E. Boerlage, M.D. Kennedy, Mp Aniye, E.M. Abogrean, D.E.Y. El-Hodali, Z.S. Tarawneh, J.C. Schippers, Modified fouling Indexultrafiltration to compare pretreatment processes of reverse osmosis feedwater, Desalination 131 (2000) 201–214.

[29] S.G. Salinas-Rodriguez, G.L. Amy, J.C. Schippers, M.D. Kennedy, The modified fouling index ultrafiltration constant flux for assessing particulate/colloidal fouling of RO systems, Desalination 365 (2015) 79–91.

[30] J.C. Schippers, J. Verdouw, The modified fouling index, a method of determining the fouling characteristics of water, Desalination 32 (1980) 137–148.

[31] ASTM standard (D 4189-07): standard test method for Silt Density Index (SDI) of water, D19.08 on Membranes and Ion Exchange Materials, 2007.

[32] S.A. Alizadeh Tabatabai, J.C. Schippers, M.D. Kennedy, Effect of coagulation on fouling potential and removal of algal organic matter in ultrafiltration pretreatment to seawater reverse osmosis, Water Res. 59 (2014) 283–294.

[33] L.O. Villacorte, Algal blooms and membrane-based desalination technology (Ph.D. thesis), UNESCO-IHE/TUDelft, Delft, 2014.

[34] L.O. Villacorte, S.A.A. Tabatabai, N. Dhakal, G. Amy, J.C. Schippers, M.D. Kennedy, Algal blooms: an emerging threat to seawater reverse osmosis desalination, Desalin. Water Treat. 55 (2015) 2601–2611.

[35] Assessing the occurrence of an algal bloom - chlorophyll-a concentration 〈http://www.waterman.hku.hk〉, 2016.

[36] U. Passow, Transparent exopolymer particles (TEP) in aquatic environments, Prog. Oceanogr. 55 (3) (2002) 287–333.

[37] R.K. Henderson, A. Baker, S.A. Parsons, B. Jefferson, Characterisation of algogenic organic matter extracted from cyanobacteria, green algae and diatoms, Water Res. 42 (2008) 3435–3445.

[38] M. Mecozzi, R. Acquistucci, V. Di Noto, E. Pietrantonio, M. Amici, D. Cardarilli, Characterization of mucilage aggregates in Adriatic and the Tyrrhenian Sea: structure similarities between mucilage samples and the insoluble fractions of marine humic substance, Chemosphere 44 (2001) 709–720.